Vibronic spectroscopy of the peroxyacetyl radical in the near IR

Y. J. Hu, H. B. Fu, and E. R. Bernstein

Citation: The Journal of Chemical Physics **124**, 114305 (2006); doi: 10.1063/1.2179428
View online: http://dx.doi.org/10.1063/1.2179428
View Table of Contents: http://aip.scitation.org/toc/jcp/124/11
Published by the American Institute of Physics

Vibronic spectroscopy of the peroxyacetyl radical in the near IR

Y. J. Hu, H. B. Fu, and E. R. Bernstein[a)]
Department of Chemistry, Colorado State University, Fort Collins, Colorado 80523-1872

(Received 28 December 2005; accepted 31 January 2006; published online 17 March 2006)

The $\tilde{A}\,^2A' \leftarrow \tilde{X}\,^2A''$ electronic transition of the peroxyacetyl radical (PA) is observed employing NIR/VUV ion enhancement, supersonic jet spectroscopy. Rotational envelope simulations yield a rotational temperature for ground state PA of ca. 55 K. *Ab initio* calculations of transition energies and vibrational frequencies for the $\tilde{A} \leftarrow \tilde{X}$ transition assist in the assignment of the observed spectrum. A number of the vibrational modes of the $\tilde{A}$ state are assigned to observed transitions (the O–O stretch 2^1, the COO bend 5^1, and the CCOO backbone bend 6^1). The calculations and mass spectra suggest that the ground state of the PA ion is repulsive. An increase in rotational linewidth of the overtone of the O–O stretch (2^1) is observed and discussed in terms of $\tilde{A}$ state dynamics. The O–O stretch anharmonicity is estimated to be 13.35 cm^{-1}. © *2006 American Institute of Physics*. [DOI: 10.1063/1.2179428]

I. INTRODUCTION

Organic peroxy radicals are suggested to be involved in a number of atmospheric processes: the production of photochemical smog, the formation and precipitation of acids, and the emission of trace species, such as carbon monoxide and volatile organic compounds.[1,2] The peroxyacetyl radical [PA, $CH_3C(O)OO$] is one of the most important atmospheric peroxy radicals, and it can react with NO_2 to form peroxyacetyl nitrate [PAN, $CH_3C(O)OONO_2$], an additional important atmospheric species that can serve as a temporary reservoir and transport molecule for NO_x.[3–5]

The vast majority of direct studies of PA employs the detection of its UV $\tilde{B}\,^2A'' \leftarrow \tilde{X}\,^2A''$ electronic transition;[6] however, despite its large absorption cross section ($\sim 10^{-18}$ cm^2), this transition is to a dissociative state, yielding little or no structure information concerning PA. The low lying electronic transition to the $\tilde{A}$ state, $\tilde{A}\,^2A' \leftarrow \tilde{X}\,^2A''$ (ca. 6000 cm^{-1}), is thus the only candidate for generation of rovibronic spectra of PA that can yield structural and bonding information. The $\tilde{A} \leftarrow \tilde{X}$ transition of organic peroxy radicals has been observed for several species employing absorption and intracavity laser studies.[7] Recently, cavity ringdown absorption studies have been reported for peroxy radicals in this region, and sharp, structured, well-resolved spectra (at 300 K) have been detected for PA.[8]

In this work flash pyrolysis, supersonic expansion, and infrared/ultraviolet ion enhancement spectroscopy techniques are employed to detect and study the PA radical $\tilde{A}\,^2A' \leftarrow \tilde{X}\,^2A''$ transition. A well-resolved vibronic spectrum of PA is obtained and *ab initio* calculations are performed to enable its assignment.

[a)]Electronic mail: erb@lamar.colostate.edu

II. EXPERIMENTAL PROCEDURES

A. Generation of the peroxyacetyl radical

PA is generated from PAN by flash pyrolysis. PAN is prepared by the acid catalyzed nitration of peracetic acid [$CH_3C(O)OOH$] in tridecane solvent. Synthesis of PAN is performed according to the method of Nielson *et al.*[9] and Gaffney *et al.*,[10] as modified by Williams *et al.*[11] The synthesis and handing of PAN is described in a previous publication from this laboratory.[12]

PA can be generated from PAN by two techniques: photolysis and pyrolysis. These two methods are typically interchangeable, generating the same radical in most, but not all instances. Our laboratory has employed both of these approaches previously to generate methoxy, benzyls, cyclopentadienyls, NCO, picolyls, and other radicals.[13]

Numerous experimental studies have shown that the thermal decomposition of PAN occurs only via a NO_2 producing channel (nitrate O–N bond cleavage),

$$CH_3C(O)O_2NO_2(PAN) \rightarrow CH_3COOO\cdot + NO_2, \qquad (1)$$

with no contribution from a NO_3 producing channel (peroxy O–O bond cleavage),

$$CH_3C(O)O_2NO_2(PAN) \rightarrow CH_3COO\cdot + NO_3, \qquad (2)$$

even though the channels are predicted to be nearly isoenergetic. It has been argued that the thermal decomposition via (1) is favored over (2) because (1) dissociation proceeds without a barrier.[12,14] Thus pyrolysis appears to be the method of choice for the generation of PA from PAN. The basic flash pyrolysis/supersonic pulsed nozzle design was first reported by Kohn *et al.*[15] Our own version of this design is described in detail previously.[12] Briefly, a 4.5 mm o.d. and a 0.8 mm i.d. alumina tube (Versus McDonald Co.) with a length of 1 in. is attached to a General Valve Series 9 pulsed solenoid valve. Both the alumina tube and the nozzle are coaxial. Heater wire (Ari Co.) is wound around the Al_2O_3 extension tube and coated with alumina cement (Cotronics

 © 2006 American Institute of Physics

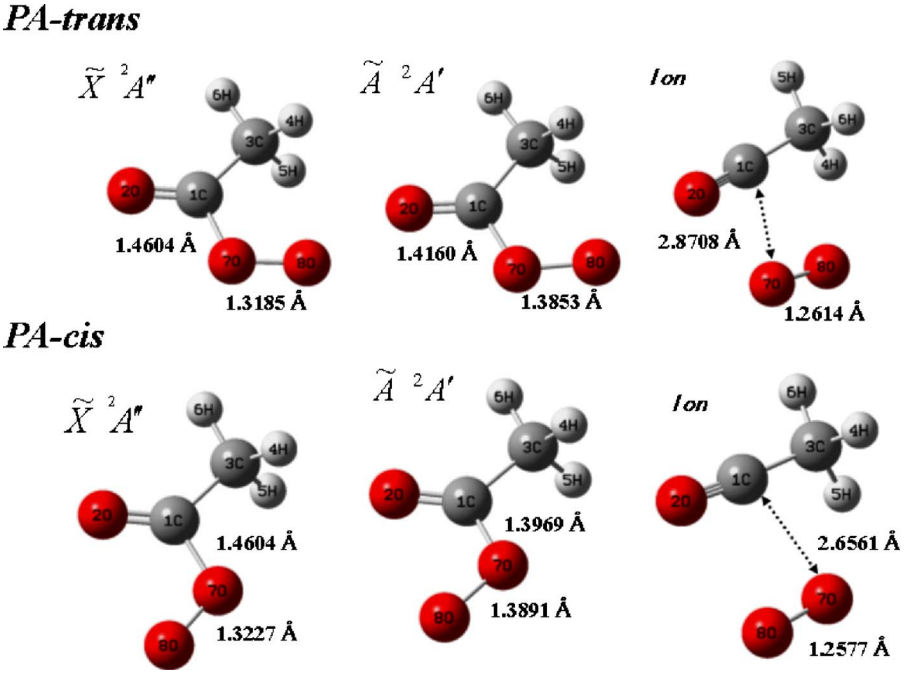

FIG. 1. (Color online) Optimized geometries of *trans* PA and *cis* PA in the ground and first excited states of the neutral and ground states of the ion states at the MP2/aug-cc-pVDZ level of theory.

Co.). A cooling system is contacted to the front flange of the nozzle to act as a heat shield that prevents slow decomposition of PAN in the body of the pulsed nozzle before it is introduced into the heated tube for flash pyrolysis.

B. NIR/VUV detection of the peroxyacetyl radicals

Employing vacuum ultraviolet (VUV) and near IR light sources, the $\tilde{A}\ ^2A' \leftarrow \tilde{X}\ ^2A''$ electronic transition of PA radicals can be detected. The ionization energy (IE) of PA is about 11 eV;[16] thus, the radicals can be ionized by employing one VUV photon (118 nm) and one near IR photon (1.54 μm). While the wavelength of VUV light is fixed, the IR/NIR laser is scanned to excite the jet-cooled radicals to their first electronic excited state ($\tilde{A}$ state). The VUV absorption of PA will be different for the ground state and the excited state (mostly the latter absorption will be increased), and ion signal intensity will be enhanced following the radical excitation. Thus, IR absorption spectra of the radicals can be recorded by using the mass resolved excitation spectroscopy (MRES) technique. VUV (118 nm) light is generated from the third harmonic of the Nd:YAG (yttrium aluminum garnet) laser (~25 mJ/pulse, maximum energy), tripled in a Xe/Ar mixture at 1:10 relative concentration for 200–500 Torr of total pressure.[12,17] Tunable IR radiation in this wavelength range (1–2 nm) can be conveniently generated with an optical parametric oscillation (OPO) pumped by 532 nm laser radiation, generated by doubling the fundamental output of a seeded Nd/YAG laser. The VUV photons (~5 μJ/pulse or $\sim 5\times 10^{12}$ photons/pulse) are focused into the vacuum chamber to ionize the radicals by single photon ionization. The nominal bandwidth of the OPO laser system output is 3 cm^{-1}. Employing an injection seeded Nd/YAG pump source and a grating tuning mirror assembly in place of the rear OPO optic reduces the IR output bandwidth further to ca. 0.4 cm^{-1}. The output power of this laser system is ~4 mJ/pulse from 1.0 to 2.1 μm. The whole time-of-flight mass spectroscopy (TOFMS)/MRES technique has been described in detail previously.[12]

C. Computational methods

To analyze and predict the observed spectra, and in general to support the study of new species, *ab initio* calculations are performed on PA using the GAUSSIAN 98 package.[18] All geometries of the species are fully optimized at the second-order Møller-Plesset perturbation (MP2) level with an aug-cc-pVDZ basis set. Energies are computed by performing single point calculations at the MP4(SDTQ)/aug-cc-pVDZ level of the theory from the geometries calculated at the MP2/aug-cc-pVDZ theory level. The first excited state of the PA is predicted by the single excitation configuration interaction (CIS)/6-31G(*d*) calculation method. Higher level calculations for geometry optimization and single point energy calculation for the excited state are also performed. Two conformers of PA exist, *trans* and *cis*. These two conformers can interconvert by O–O internal rotation around the C–O bond; the energy of the *trans* form is lower by ca. 300 cm^{-1} than the *cis* form.[8] The *trans* PA conformer is thought to be the only one populated in the supersonic jet experiment. Harmonic frequency calculations for the *trans* PA conformer at the MP2/aug-cc-pVDZ level of theory are also performed for both $\tilde{X}$ and $\tilde{A}$ states.

III. RESULTS AND DISCUSSION

A. Calculations

The structures of *cis* and *trans* PA in the $\tilde{X}\ ^2A''$ state, the $\tilde{A}\ ^2A'$ states, and the ground state of the ion are shown in Fig. 1. The optimized geometries indicate that the electronic excitation $\tilde{A}\ ^2A' \leftarrow \tilde{X}\ ^2A''$ mainly induces the following changes in geometry: $\Delta R_{C1-O7} = -0.045$ Å, $\Delta R_{C7-O8} = 0.067$ Å for

TABLE I. Energies of PA based on *ab initio* calculations at MP4(SDTQ)/aug-cc-pVDZ level of theory using the geometry calculated at the MP2/aug-cc-pVDZ level of theory.

Isomers	Vertical IE (eV)	Adiabatic IE (eV)	T_e (cm^{-1})	T_{0-0} (cm^{-1})	$\Delta E_{trans\text{-}cis}$ (cm^{-1})[a]
Trans	10.8	9.2	6690	5659	325
Cis	11.7	9.1			

[a]Difference in energies of PA between *trans* and *cis* conformers in the ground state.

trans PA; and $\Delta R_{C1-O7}=-0.064$ Å, $\Delta R_{C7-O8}=0.066$ Å for *cis* PA. The results suggest that the terminal O–O bond is most changed in the vibronic transition $\tilde{A}\,^2A' \leftarrow \tilde{X}\,^2A''$; however, vibrational frequency calculations for the $\tilde{A}\,^2A'$ state of the *cis* PA at the MP2/aug-cc-pVDZ level of theory yield one imaginary frequency. This suggests that *cis* PA on the excited *A* state is a first-order saddle point and thus not a stable structure (at this level of theory). PA on the ion ground state surface has its terminal O–O moiety far from the rest of the radical and the separation of these two oxygen atoms decreases. Based on these calculations, the PA ion ground state is obviously a repulsive state and will generate the CH_3CO^+ radical ion and O_2 molecule.

Given these geometry results for the optimized structures of the $\tilde{X}$ and $\tilde{A}$ states of PA, the vibrational modes 2 (O–O stretch), 5 (COO bend), and 6 (CCOO backbone bend) should have significant intensity in the $\tilde{A} \leftarrow \tilde{X}$ vibronic structure.

Table I summarizes the results of the single point energy calculations for PA. The calculated transition energy for the *trans* PA conformer is predicted to be ca. 5659 cm^{-1}, which is close to the observed value of 5582.5 cm^{-1}.[8] Thus, the predicted energies calculated at the MP4(SDTQ)/aug-cc-pVDZ level of theory using geometries calculated at the MP2/aug-cc-pVDZ level of theory are believable. The adiabatic IEs for both *trans* and *cis* PA are predicted as 9.1 and 9.2 eV, respectively. The calculated vertical IEs, which are the important quantities related to photoionization, are 10.8 eV for *trans* and 11.7 eV for *cis* PA, respectively. The electronic excitation energy (T_e) for *trans* PA is predicted to be higher by ca. 1000 cm^{-1} than the $\tilde{A} \leftarrow \tilde{X}$ origin transition (T_{00}) (see Table II).

B. Experiments

1. Observation of the spectra

The species generated by thermal decomposition of PAN and expanded in the vacuum system through the supersonic nozzle are photoionized by VUV (118 nm) light and detected

TABLE II. Assignment of the vibronic $\tilde{A}\,^2A' \leftarrow \tilde{X}\,^2A''$ spectrum of PA (cm^{-1}).

Expt.					
Peak position	$\nu_i - 0_0^0$	*Ab initio*[a]	Vibration mode in $\tilde{A}\,^2A'$ excited state	Intensity[b]	Comments
5582.5	0			*s*	T_{00}
5735.5	153			*w*	C–H stretch[c]
5756	173.5			*w*	C–H stretch[c]
5815	232.5			*w*	C–H stretch[c]
5852.3	269.8	269	7^1 backbone	*w*	
5883	300.5			*w*	C–H stretch[c]
6055.9	473.4	443	6^1 CCOO backbone	*m*	
6120.6	538.1	510	5^1 COO bend	*m*	
6208.1	625.6		Hot band	*w*	Uncertain
6342.4	759.9	729	4^1 backbone	*w*	
6424	841.5	932	3^1 backbone	*w*	
6510.9	928.4	1079	2^1 O–O stretch	*s*	Vertical excitation
6593.6	1011.1		$5^1\,6^1$	*w*	Uncertain
6631	1048.5		5^2	*w*	Uncertain
6660.2	1077.7		Hot band	*w*	Uncertain
6726.3	1143.8	1104	1^1 backbone	*m*	
6777.4	1194.9		$2^1\,7^1$	*w*	Uncertain
6806	1223.5		$4^1\,5^1$	*w*	Uncertain
6978.2	1395.7		$2^1\,6^1$	*m*	
7015.1	1432.6		$3^1\,5^1$	*w*	Uncertain
7041	1458.5		$2^1\,5^1$	*m*	
7412.7	1830.1		2^2	*s*	
7954.4	2371.9		$2^2\,5^1$	*w*	

[a]Calculated at MP2(FC)/aug-cc-pVDZ level of theory, scaled by 0.937.
[b]Intensity: *s*: strong, *m*: medium, and *w*: weak.
[c]C–H stretch first overtone in the ground state.

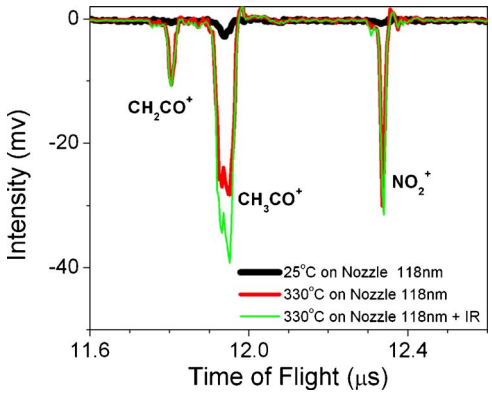

FIG. 2. (Color online) TOFMS of PAN and PA decomposition products photoionized (1+1) by 118 nm+near IR light.

by time of flight mass spectrometry. Three main features are present in this mass spectrum at m/z values of 42, 43, and 46 (see Fig. 2): they are assigned as CH_2CO^+, CH_3CO^+, and NO_2^+, respectively. With the nozzle at room temperature, these three features are very weak and probably arise from the photodissociation of PAN by VUV light. When the tube attached to the nozzle is heated, intensities of the three peaks increase simultaneously. The species CH_2CO (ketene) arises from the thermal decomposition of PA.[14] Thermal decomposition mechanisms for PA are discussed in a previous report from this laboratory.[12] Both IEs of CH_2CO and NO_2 are below 10 eV [9.64 eV (Ref. 19) for CH_2CO and 9.60 eV (Ref. 20) for NO_2] and both can be ionized by a single photon of VUV light. Photochemical processes are different for PA, however. *Ab initio* calculations predict that the vertical IE of the *trans* PA is 10.8 eV (the absolute maximum error is ca. 0.4 eV),[21] which is consistent with the reported data.[16] Thus, a single VUV (118 nm) photon is possibly sufficient for the ionization of PA, although this energy is just at threshold. Optimized geometries of PA in the ground state, the first excited state, and the ground state of the ion (Fig. 1) suggest that the PA in the ground state and first excited state have similar geometries; however, the PA ion ground state is repulsive, implying that the PA parent ion will not be observed. The mass spectra support the above analysis. The broad peak corresponding to CH_3CO^+ can only be observed when the pyrolysis nozzle is heated. Compared to the TOFMS features for CH_2CO and NO_2, the peak FWHW for CH_3CO is broad (10 vs 45 ns). This suggests that PA is fragmented following the ionization by a single VUV (118 nm) photon. With the temperature of the pyrolysis nozzle kept at 330 °C, tuning the OPO laser light to vibronic resonances within the $\tilde{A}\,^2A' \leftarrow \tilde{X}\,^2A''$ transition increases the intensity of CH_3CO peak by as much as 30%, while the others remain constant.

Thus we conclude that only the CH_3CO radical signal relates to the photodissociation (at ionization) of PA.

As discussed above, the energy of one VUV photon is just at the ionization threshold of PA and an added IR photon energy to a PA should increase the ionization cross section. Figure 3 shows the $\tilde{A}\,^2A' \leftarrow \tilde{X}\,^2A''$ vibronic transition spectrum of PA in the near IR, obtained by monitoring CH_3CO^+, the mass channel, and scanning the IR laser, with the 118 nm

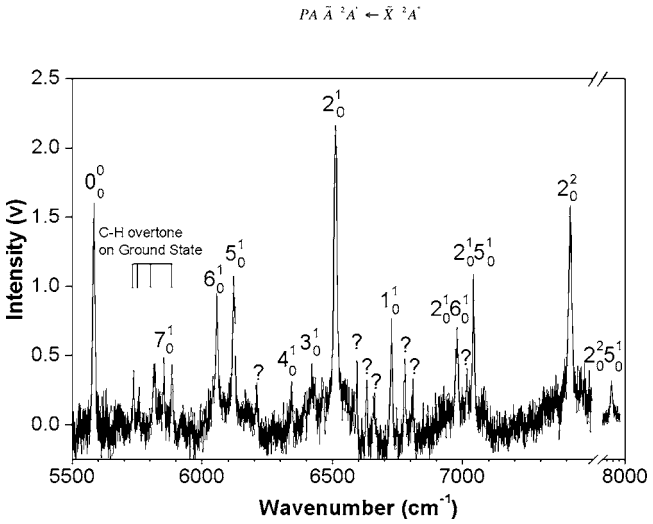

FIG. 3. Spectrum of the $\tilde{A}\,^2A' \leftarrow \tilde{X}\,^2A''$ vibronic transition of PA in the near IR. The spectrum is detected in CH_3CO^+ mass channel. *Ab initio* calculations are employed to assign the spectrum.

laser fixed to ionize PA. The spectrum shows a strong absorption at 5582.5 cm^{-1} that corresponds to the origin transition of the $\tilde{A}\,^2A' \leftarrow \tilde{X}\,^2A''$ electronic transition of *trans* PA. Our result is consistent with the report of Zalyubovsky *et al.*[8] Simulated rotational contours of the transition (SPECVIEW software package[22]) yield a rotational temperature for PA in the supersonic jet of roughly 55 K (see Fig. 4).

2. Spectrum assignment and analysis

Only the transitions to symmetric modes in the $\tilde{A}$ state are allowed from the vibrationless level of the $\tilde{X}$ state. The unpaired electron for the PA radical is localized on the terminal oxygen, and thus, modes involved with the motion of the terminal oxygen are expected to be most active for this transition. We can assign most of the individual peaks in the PA $\tilde{A} \leftarrow \tilde{X}$ spectrum based on this assumption.

Assignment of the spectrum employing *ab initio* calculations for the vibrational modes of the $\tilde{A}$ state are shown in Fig. 3 and Table II. *Ab initio* calculations suggest that the transition from the ground electronic state to the O–O stretching vibration (2^1) in the $\tilde{A}$ state will be an important vibronic feature for vertical excitation. The frequency of this vibrational mode is calculated as ca. 1080 cm^{-1}. In the spectrum shown in Fig. 3, a strong peak located at 6511 cm^{-1} and shifted from the origin by 928.4 cm^{-1} can be assigned as the O–O stretch (2^1) in the $\tilde{A}$ state. Similarly, another strong peak located at 7413 cm^{-1}, separated from the origin by ca. 1830 cm^{-1}, is suggested to be the overtone of this O–O stretch (2^2) in the $\tilde{A}$ state.

Two more features that can be identified in the spectrum are associated with the COO (5^1) bend and CCOO (6^1) backbone vibrational modes in the excited state. The former is located at ca. 6121 cm^{-1}, shifted from the origin by ~538 cm^{-1} and the latter is at ca. 6056 cm^{-1}, separated from the origin by 473 cm^{-1}. These two energies of the observed 5^1 and 6^1 modes are in good agreement with the calculations

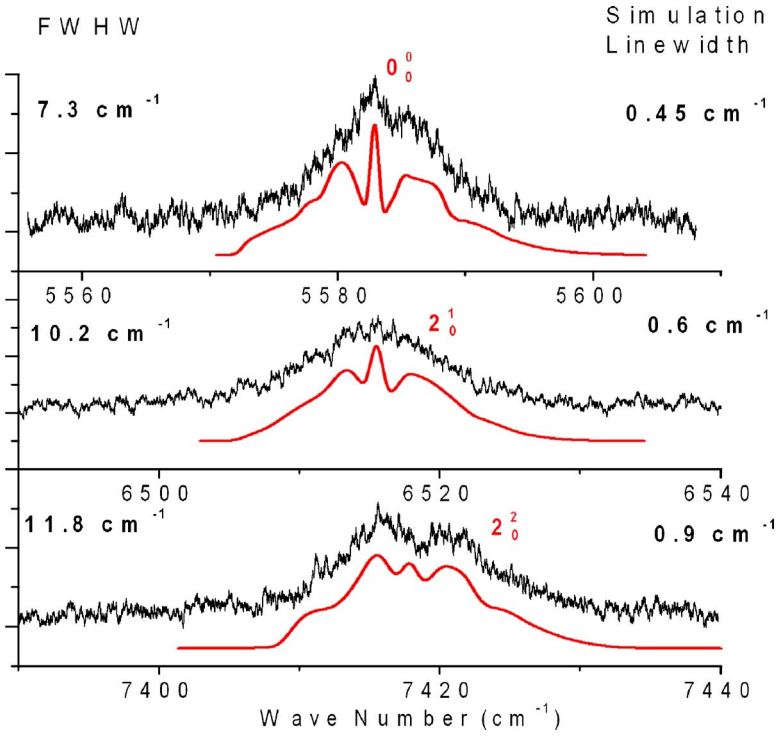

FIG. 4. (Color online) Spectra of the 0_0^0, 2_0^1, and 2_0^2 electronic transitions of PA and their simulated rotational contours. Simulation results give the rotational temperature of PA generated in the nozzle as ca. 55 K.

(see Table II). Further confirmation of these assignments comes from another two medium intensity peaks located at ca. 6978 and 7041 cm^{-1}. These are assigned as the combination bands $2^1 6^1$ and $2^1 5^1$, respectively. Combination band $2^2 5^1$ can also be assigned in the spectrum located at ca. 7954 cm^{-1}. Weaker features, whose assignments became less certain, are also observed in the spectrum. With the assistance of *ab initio* calculations, the peak at 5852 cm^{-1} can be assigned as due to the CCOO backbone mode (7^1). The peaks located at 6342, 6424, and 6726 cm^{-1} are assigned as the other backbone modes (4^1, 5^1, and 1^1, respectively) of PA in the $\tilde{A}$ state. The other weak features of the $\tilde{A} \leftarrow \tilde{X}$ transition are likely due to combination bands and hot bands. All possible assignments are listed in Table II. Based on *ab initio* calculations for the ground state of PA, the four additional weak bands observed around 5800 cm^{-1} may be associated with C–H overtones of the ground state, as no more active vibrational modes can be assigned for the excited state around that energy.

3. 2^2 O–O stretch overtone in the $\tilde{A}$ state

Figure 4 shows the observed and simulated rotational contours for the 0_0^0, 2_0^1, and 2_0^2 transitions of the $\tilde{A} \leftarrow \tilde{X}$ PA transition.[22] Table III lists the rotational constants of the *trans* PA ground state and excited state obtained from *ab initio* calculations. These values are used in the simulation analysis. For these three spectral features (0_0^0, 2_0^1, and 2_0^2), the FWHW of the bands are 7.3, 10.2, and 11.8 cm^{-1}, respectively. The linewidths of the simulated rotational contours for these transitions increase from 0.45 to 0.9 cm^{-1}. The IR laser linewidth is ~0.4 cm^{-1} for all these features. Similar linewidth results for overtone fractures are reported by Wei and Reisler[23] for the O–H stretch mode of the CH_2OH radical $\tilde{X}$ state. Three possibilities can be considered as the cause of this increased rotational linewidth: (1) homogeneous (dynamical) broadening, as observed for the OH stretch second overtone in methanol and hydroxylamine;[24,25] (2) spectral overlap of a few sharp transitions involving mixed states that borrow oscillator strength from the O–O overtone; and (3) possible change in the upper state rotational constants at higher energy. Due to the bandwidth (~0.4 cm^{-1}) of the IR laser radiation and the lack of further information on PA, these three possibilities cannot be readily distinguished.

TABLE III. *Ab initio* calculated rotational constants (cm^{-1}) for *trans* PA (MP2/aug-cc-pVDZ level of theory).

States	A	B	C
Excited state ($\tilde{A}$)	0.312 125	0.158 261	0.107 154
Ground state ($\tilde{X}$)	0.305 770	0.160 405	0.107 336

For the O–O stretching vibration of PA in the $\tilde{A}$ state, the energies for the fundamental and first overtone should follow the Birge-Sponer relation: $\Delta\nu/v = A + Bv$, where $\Delta\nu$ is the transition frequency in wave numbers (928.4 and 1830.1 cm^{-1}), v is the quantum number of the stretching vibration ($v=1,2$), $(A-B)$ is the harmonic or mechanical energy of mode 2^1, and $-B$ is the anharmonicity.[24] The 2^1 O–O stretch anharmonicity for PA in the $\tilde{A}$ state can thus be estimated as 13.35 cm^{-1} in this work and $A=941.75$ cm^{-1}. (Note that $\omega_e = A - B = 941.75 + 13.35$ $cm^{-1} = 955.1$ cm^{-1} and that $\omega_e x_e = -B = 13.35$ cm^{-1}.)

IV. CONCLUSION

The $\tilde{A}\,^2A' \leftarrow \tilde{X}\,^2A''$ electronic transition of the peroxyacetyl radical using NIR/VUV ion enhancement spectros-

copy is observed and analyzed. Rotational envelope simulations show that the rotational temperature for PA in the ground state is ca. 55 K.

Ab initio calculations are performed on the PA radicals. The transition energies and the vibrational frequencies for the $\tilde{A} \leftarrow \tilde{X}$ transition and the $\tilde{A}$ state are calculated to assist in the assignment of the spectrum. Vibronic transitions involving the O–O stretch 2^1, COO bend 5^1, and CCOO backbone 6^1 modes are identified. Geometry optimization calculations and mass spectra suggest that the ion ground electronic state of PA is a repulsive state. An increase in rotational linewidth of the overtone of the O–O stretch is observed and discussed. The O–O stretch anharmonicity in the $\tilde{A}$ state is estimated at 13.35 cm^{-1}.

ACKNOWLEDGMENTS

This work was supported in part by the NSF and by Philip Morris USA.

[1] J. G. Calvert, A. Lazrus, G. L. Kok, B. G. Heikes, J. G. Walega, J. Lind, and C. A. Cantrell, Nature (London) **317**, 27 (1985).
[2] M. Claeys, B. Graham, G. Vas *et al.*, Science **303**, 1174 (2004).
[3] H. B. Singh and L. J. Salas, Nature (London) **302**, 326 (1983).
[4] W. J. Moxim, H. Levy, and P. S. Kasibhatla, J. Geophys. Res. **101**, 12621 (1996).
[5] C. Bruhl, U. Poochl, P. J. Cratzen, and B. Steil, Atmos. Environ. **34**, 3431 (2000).
[6] P. D. Lightfoot, R. A. Cox, J. N. Crowley, M. Destriau, G. D. Hayman, M. E. Jenkin, G. K. Moortgat, and F. Zabel, Atmos. Environ. **26A**, 1805 (1992).
[7] H. E. Hunziker and H. R. Wendt, J. Chem. Phys. **64**, 3488 (1976).
[8] S. J. Zalyubovsky, B. G. Glover, and T. A. Miller, J. Phys. Chem. A **107**, 7704 (2003).
[9] T. Nielsen, A. M. Hansen, and E. L. Thomsen, Atmos. Environ. **10**, 115 (1982).
[10] J. S. Gaffney, R. Fajer, and G. I. Senum, Atmos. Environ. **18**, 215 (1984).
[11] J. Williams, J. M. Roberts, and S. B. Bertman, J. Geophys. Res. **105**, 28943 (2000).
[12] Y. J. Hu, H. B. Fu, and E. R. Bernstein, J. Phys. Chem. A (to be published).
[13] Q. Y. Shang, P. O. Moreno, and E. R. Bernstein, J. Am. Chem. Soc. **116**, 311 (1994); Q. Y. Shang and E. R. Bernstein, J. Chem. Phys. **100**, 8625 (1994); R. Disselkamp, E. R. Bernstein, J. I. Seeman, and H. V. Secor, *ibid.* **97**, 8130 (1992).
[14] S. von Ahsen, H. Willner, and J. S. Francisco, J. Chem. Phys. **21**, 2048 (2004).
[15] D. W. Kohn, H. Clauberg, and P. Chen, Rev. Sci. Instrum. **63**, 4003 (1992).
[16] M. Litorja and B. Ruscic, J. Electron Spectrosc. Relat. Phenom. **97**, 131 (1998).
[17] D. N. Shin, Y. Matsuda, and E. R. Bernstein, J. Chem. Phys. **120**, 4157 (2004).
[18] M. J. Frisch, G. W. Trucks, H. B. Schlegel *et al.*, GAUSSIAN 03, Revision B.02, Gaussian, Inc., Pittsburgh, PA, 2003.
[19] H. Bock, T. Hirabayashi, and S. Mohmand, Chem. Ber. **114**, 2595 (1981).
[20] D. E. Clemmer and P. B. Armentrout, J. Chem. Phys. **97**, 2451 (1992).
[21] J. B. Foresman and A. Frisch, *Exploring Chemistry with Electronic Structure Methods: A Guide to Using Gaussian*, 2nd ed. (Gaussian Inc., Pittsburgh, PA, 1998).
[22] V. L. Stakhursky, http://molspect.mps.ohio-state.edu/goes/specview.html
[23] L. F. Wei and H. Reisler, J. Phys. Chem. A **108**, 7903 (2004).
[24] O. V. Boyarkin, L. Lubich, R. Settle, D. Perry, and T. Rizzo, J. Chem. Phys. **107**, 8409 (1997).
[25] J. L. Scott, D. Luckhaus, S. S. Brown, and F. F. Crim, J. Chem. Phys. **102**, 675 (1995).